Excess Light Priming in *Arabidopsis thaliana* Genotypes with Altered DNA Methylomes

Diep R. Ganguly,[1] Bethany A. B. Stone,[1] Andrew F. Bowerman, Steven R. Eichten, and Barry J. Pogson[2]

Australian Research Council Centre of Excellence in Plant Energy Biology, Research School of Biology, The Australian National University Canberra, Acton, ACT, 2601, Australia

ORCID IDs: 0000-0001-6746-0181 (D.R.G.); 0000-0003-3246-7943 (B.A.B.S.); 0000-0003-1729-7843 (A.F.B.); 0000-0003-2268-395X (S.R.E.); 0000-0003-1869-2423 (B.J.P.)

ABSTRACT Plants must continuously react to the ever-fluctuating nature of their environment. Repeated exposure to stressful conditions can lead to priming, whereby prior encounters heighten a plant's ability to respond to future events. A clear example of priming is provided by the model plant *Arabidopsis thaliana* (Arabidopsis), in which photosynthetic and photoprotective responses are enhanced following recurring light stress. While there are various post-translational mechanisms underpinning photoprotection, an unresolved question is the relative importance of transcriptional changes toward stress priming and, consequently, the potential contribution from DNA methylation – a heritable chemical modification of DNA capable of influencing gene expression. Here, we systematically investigate the potential molecular underpinnings of physiological priming against recurring excess-light (EL), specifically DNA methylation and transcriptional regulation: the latter having not been examined with respect to EL priming. The capacity for physiological priming of photosynthetic and photoprotective parameters following a recurring EL treatment was not impaired in Arabidopsis mutants with perturbed establishment, maintenance, or removal of DNA methylation. Importantly, no differences in development or basal photoprotective capacity were identified in the mutants that may confound the above result. Little evidence for a causal transcriptional component of physiological priming was identified; in fact, most alterations in primed plants presented as a transcriptional 'dampening' in response to an additional EL exposure, likely a consequence of physiological priming. However, a set of transcripts uniquely regulated in primed plants provide preliminary evidence for a novel transcriptional component of recurring EL priming, independent of physiological changes. Thus, we propose that physiological priming of recurring EL in Arabidopsis occurs independently of DNA methylation; and that the majority of the associated transcriptional alterations are a consequence, not cause, of this physiological priming.

Plants must respond to various stresses imposed by their environment. Abiotic stresses may occur over long periods of development with unfavorable conditions persisting stably as is characteristic of extreme climates. Alternatively, environments can be highly dynamic and comprise of transient, often recurring, stressful events. Information processing is key for effective physiological and developmental responses to specific environmental factors. Indeed, there is growing evidence that plants can 'remember' past experiences (Hilker *et al.* 2016). In addition to long-term acclimation to sustained environmental changes, short-term plant stress responses are modified by prior exposure to a transient, and often recurring, specific environmental stimulus (referred to as priming). Here, the future fitness of a primed individual is increased by reducing the damage of stressful events, while the costs of initiating and maintaining priming are outweighed by the costs of stress exposure in an 'un-primed' (or naive) state (Hilker *et al.* 2016).

A variety of mechanisms have been reported to contribute toward stress priming including transcriptional memory underpinned by stalled

RNA Pol II and elevated H3K4me3 (Ding *et al.* 2012), and fractionation of H3K27me3 patterns (Sani *et al.* 2013). It has also been reported that the activity of the HSFA2 transcription factor can result in H3K4me2 and H3K4me3 changes, in response to recurring heat stress, to convey transcriptional priming (Lämke *et al.* 2016). Additionally, HDA6-mediated histone H4 de-acetylation has been linked to prime jasmonic acid signaling leading to enhanced drought tolerance (Kim *et al.* 2017). These various examples highlight the importance of chromatin variation in facilitating of plant stress priming. Another chromatin mark speculated to promote priming is DNA methylation, variations in which could, theoretically, be stably inherited over mitotic cell divisions to convey persistent transcriptional control (Johannes and Schmitz 2019). The targeting of the RNA-directed DNA methylation (RdDM) pathway toward promoter regions of genes, and the occurrence of gene body methylation (gbM), suggests that differential methylation could arise within genes or their regulatory elements to cause functional differences (Matzke and Mosher 2014; Bewick *et al.* 2016). Such observations highlight the potential regulatory capacity for DNA methylation.

An extant question is the exact regulatory potential of DNA methylation. Canonically, DNA methylation is considered a mechanism for transcriptional repression, for example through steric hindrance of RNA polymerase II (Molloy 1986). This silencing is most pronounced at transposable elements (TEs) (Cokus *et al.* 2008). On the other hand, gbM is often found within constitutively expressed genes although there is conflicting evidence for an effect on transcription (Bewick *et al.* 2016; Muyle and Gaut 2019). Other reports implicate the involvement of DNA methylation in alternative splicing and modulation of transcription factor binding capacity (Shukla *et al.* 2011; O'Malley *et al.* 2016; Yin *et al.* 2017). Given these various mechanisms, and placing DNA methylation in the broader context as being one of many chromatin modifications, it might be unsurprising that efforts to quantify the contribution of DNA methylation, at an organism level, toward transcription have shown a weak relationship (Meng *et al.* 2016). Instead, changes in the methylome may be a consequence of gene expression changes rather than a driver (Secco *et al.* 2015). The ability to identify causative changes in the methylome are further complicated as the effects of DNA methylation can be in both *cis* and *trans* (Rowley *et al.* 2017).

Given these complications, various tools exist to quantify the effects of variable methylation (epi-alleles) on, and in response to, gene expression and physiological traits. The utilization of epigenetic recombinant inbred lines that display variable methylation patterns, but are isogenic, demonstrated that epi-alleles could contribute toward quantifiable phenotypic differences (Johannes *et al.* 2009; Cortijo *et al.* 2014). Mutants with defective methylation machinery that exhibit a variety of methylome variations, depending on the severity of the mutation, have also been used to correlate a relationship between DNA methylation and plant stress responses (Boyko *et al.* 2010; Le *et al.* 2014; Wibowo *et al.* 2016). Mutants are also described to be developmentally or morphologically aberrant, however, it is not clear whether this is the direct result of methylation changes or an indirect effect of TE de-regulation and genomic instability (Finnegan *et al.* 1996; Reinders *et al.* 2009; Stroud *et al.* 2014; Williams and Gehring 2017). Indeed, traits attributed toward methylome variants could equally be tied to underlying TE activity (Ong-Abdullah *et al.* 2015; Wibowo *et al.* 2016; He *et al.* 2018).

We previously demonstrated that Arabidopsis is primed by a recurring EL regime, evident by altered non-photochemical quenching (NPQ) and improved photosystem II (PSII) efficiency (Ganguly *et al.* 2018). However, we detected no associated changes in DNA methylation.

While this demonstrated that the Arabidopsis methylome was impervious to recurring EL, it does not preclude transcriptional regulation of EL priming to which appropriate methylome maintenance may be important. In fact, EL-exposed tissue can promote the induction of EL-responsive transcripts in naive leaves for added photoprotection through the process of systemic acquired acclimation (SAA) (Karpinski 1999; Rossel *et al.* 2007; Gordon *et al.* 2012). As the methylation machinery was operational during previous analyses, any light-induced changes may have been reset prior to tissue harvesting. Indeed, the disruption of methylation pathways has revealed transgenerational effects that were otherwise reset (Iwasaki and Paszkowski 2014). Thus, we sought to clarify these unknowns by testing whether a range of mutants, which are unable to maintain or reset their methylome, were capable of priming against recurring EL; and subsequently characterizing differences in the transcriptome of EL primed plants. We report that DNA methylation mutants display functional photoprotection and EL priming to an equivalent extent as wild-type plants (WT; Col-0). Furthermore, while primed plants demonstrate a completely reset transcriptome, they also displayed attenuated responses to further EL, which we refer to as "dampening", potentially reflecting the reduced generation of stress signaling molecules due to enhanced photoprotection.

MATERIALS AND METHODS

Plant growth and germplasm

All *Arabidopsis* germplasm utilized were in the Columbia (Col-0) background. Plant lines comprised of wild-type Col-0 (WT), *ddc* (CS16384; *drm1-2 drm2-2 cmt3-*11), *strs2* (SALK_028850), and *rdd* (derived from *ros1-4*, SALK_045303; *dml2*, SALK_131712; *dml3-2*, SALK_056440). All seeds were obtained from the Arabidopsis Biological Research Centre (Ohio State University, Columbus, OH, USA), with the exception of *rdd* which was kindly provided by Dr. Ming-Bo Wang (CSIRO, Canberra, Australia) (Le *et al.* 2014). Primers used for genotyping are listed in Supplementary Dataset 8.

For plant growth, Arabidopsis seeds were sown onto individual pots containing moist Seed Raising Mix (Debco, NSW, Australia). Soil was supplemented with Osmocote Exact Mini slow release fertilizer (Scotts, NSW, Australia) at a concentration of 1 g/L dry volume of soil and treated with 1 L of 0.3% (v/v) AzaMax (OCP, NSW, Australia) prior to sowing to prevent insect infection. Seeds were covered with clear plastic wrap and stratified at 4° in the dark for at least 72 hr to break dormancy and coordinate germination. Stratified seeds were transferred to a temperature controlled Conviron S10H growth chamber (Conviron, Winnipeg, MB, Canada) for cultivation under standard growth conditions: 12-hour photoperiod (08:00-20:00), 100-150 μ mol photons m^{-2} s^{-1}, 20° ($\pm$ 2°), 55% ($\pm$ 5%) relative humidity. Upon germination, clear plastic wrap was slowly removed over 7-10 days, to maintain high humidity until seedlings were well-established and to avoid humidity shock. Plants were watered every 2-3 days depending on soil moisture, avoiding pooling of water to prevent algal and fungal growth. Each of three daily EL treatments consisted of 60 min of 1000 μ mol photons m^{-2} s^{-1} using a mixture of metal halide and high-pressure sodium lamps as previously described (Crisp *et al.* 2017; Ganguly *et al.* 2018).

For MethylC- and mRNA-seq experiments, developmentally equivalent leaves were harvested in biological triplicate (three independent plants per time-point or genotype) to make comparisons (true leaves 4 - 9 in order of emergence). Harvested tissue was flash-frozen in liquid N$_2$ and ground into a fine powder using a 1/8″ steel ball bearing, in a 1.5 ml Eppendorf tube, with 1 min shaking at 25 Hz in the *Tissue Lyser II* (Qiagen, Hilden, Germany). Ground tissue was stored at -80°. Approximately

20 and 30 mg of ground tissue was used for extracting total RNA and genomic DNA, respectively. MethylC-seq of WT and *strs2* was performed on paired tissue samples by using aliquots of ground frozen tissue from the same harvested plant.

High-throughput phenotyping

For all genotypes the development of 10-day old (post-germination) Arabidopsis seedlings was followed for 20 days (until 4-weeks of age) by measuring plant area and rosette compactness. The *PlantScreen Compact System* (Photon Systems Instruments, Brno, Czech Republic), a high-throughput platform for digital plant phenotyping, was used to measure plant area and rosette compactness at 08:00 daily. Images were analyzed using the *PSI RGB-IR Analyzer* software (version 1.0.0.2; Photon Systems Instruments, Brno, Czech Republic). Program settings were adjusted as needed to achieve well-defined plant areas and minimize background noise. The total number of macroscopically visible true leaves (cotyledons excluded) per rosette were also manually counted daily.

Monitoring PSII performance using chlorophyll fluorescence measurements

PSII photochemistry was probed *in vivo* using measures of chlorophyll fluorescence (Baker 2008) using a PSI FluorCam (Photon System Instruments; Brno, Czech Republic). Measures were taken between 11:00-14:00 across the adaxial side of 30 min dark adapted rosettes as performed previously (Ganguly *et al.* 2018). In this study, intermittent measures of chlorophyll fluorescence, specifically F_t, F_m, and F_m', were taken after a saturating pulse (3000 μ mol photons m^{-2} sec^{-1}) across 10-minutes in actinic light (700 μ mol photons m^{-2} sec^{-1}) followed by a 4-minute dark period (https://goo.gl/RuYDE2). The resulting fluorescence images were analyzed using the FluorCam 7 software (v1.1.1.4; Photon System Instruments, Brno, Czech Republic). Chlorophyll fluorescence signals were analyzed across whole rosettes. To better quantify light energy partitioning between photochemistry, light-regulated thermal dissipation, and other non-light induced quenching, such as chlorophyll fluorescence, we adopted the yield terms of ΦPSII, ΦNPQ, and ΦNO, which sum to unity and do not require measures of F_o (Hendrickson *et al.* 2004; Kramer *et al.* 2004).

MethylC sequencing

Genomic DNA was extracted from ground tissue using the *DNeasy Plant Mini Kit* (Qiagen, Netherlands) according to the manufacturer's instructions, and quantified using a *ND-1000* Spectrophotometer. 70 ng of *Covaris* sheared gDNA (average fragment size = 200 bp) was bisulfite converted using the *EZ DNA Methylation-Gold Kit* (Zymo Research, CA, USA) according to the manufacturer's instructions. Bisulfite converted DNA was used to create dual-indexed MethylC-seq libraries using the *Accel-NGS Methyl-Seq DNA Library Kit* paired with the *Accel-NGS Methyl-Seq Dual Indexing Kit* (Swift Biosciences, MI, USA) according to manufacturers' instructions. All libraries were amplified in a 7-cycle indexing PCR reaction. All clean-ups were performed using either *AMPure XP beads* (Beckman Coulter, CA, USA) or *Sera-mag SpeedBeads* (GE Healthcare, Buckinghamshire, UK). A *LabChip GXII* (Perkin Elmer, MA, USA) was used to determine library molarity and fragment size distribution. Libraries were pooled in equimolar ratios and sequenced on one *HiSeq2500* flow cell (100 bp single-end) at the *ACRF Biomolecular Research Facility* (Australian National University, ACT, Australia). In-depth details of library preparation are also described on protocols.io (https://goo.gl/vfwtEU).

Raw reads were quality controlled using *FastQC* (v0.11.2) with reads filtered and trimmed using *Cutadapt* (v1.9) and *Trim Galore!* (v.0.3.7) under default parameters. Single-end alignments of trimmed raw reads were aligned to the TAIR10 reference using *Bismark* (v0.14.5) (Krueger and Andrews 2011) and *Bowtie2* (v2.2.9) (Langmead and Salzberg 2012) with the flags -N 0 and -L 20. Per cytosine methylation levels were calculated using *Bismark methylation extractor* with default settings. Only cytosines with read depth > 3X were retained for further analysis. Bisulfite conversion efficiency was calculated as the proportion of methylated cytosines in the CHH context within the chloroplast genome, which itself should be fully unmethylated. Alignment metrics are provided in Supplementary Dataset 1. Weighted methylation levels were used to calculate the proportion of CG, CHG, and CHH methylation to account for sequencing depth (Schultz *et al.* 2012). This output was binned into 50 kbp regions (filtered for read depth > 15X) across the genome to construct chromosomal level metaplots of methylation levels using *BEDTools* (Quinlan and Hall 2010).

Weighted methylation levels at single cytosines was utilized in DMR identification using *DSS* (v2.28.0) with default settings, including smoothing (*smoothing span* = 100) to improve methylation estimates (Feng *et al.* 2014; Wu *et al.* 2015). Differentially methylated cytosines (DMCs) were called (*DMLtest*) based on the posterior probabilities (q-value < 0.05) for a threshold in methylation difference (*delta*) at each cytosine in a context-specific manner: 0.5 CG, 0.2 CHG, and 0.1 CHH. Subsequently, DMRs are called based on adjacent statistically significant DMCs (*callDMR* with default parameters). These were refined by removing regions with a merged test statistic (*areaStat*) and estimated methylation difference in the lowest quartile, per sequence context, to minimize stochastic DMRs and those containing DMCs of opposite direction. The final list of DMRs were assigned genomic positions, or overlapped between comparisons, using *BEDTools* and the *Araport11* annotation (Quinlan and Hall 2010; Cheng *et al.* 2017). Code used for analyses are available on *Github* (https://goo.gl/wsQrJT).

DRM1/2-dependent RdDM sites were determined as the CHH hypo-DMRs identified in common between *drm1drm2* and three independent WT samples using *DSS* with the same parameters used herein (Stroud *et al.* 2015).

mRNA sequencing

Total RNA was extracted with *TRIzol* (Life Technologies) using an adapted protocol (Allen *et al.* 2010). Briefly, ground tissue was lysed in 1 ml *TRIzol* and mixed by gentle inversion and incubated at room temperature for 5 min. Subsequently, 200 μl chloroform was added and shaken vigorously to mix. Samples were centrifuged at 14,000 rcf for 10 min at 4° to separate the resulting upper aqueous phase from the organic phase. Chloroform extraction was repeated twice, transferring 400-600 μl then 300-400 μl aqueous phase to a new microfuge tube following each extraction. RNA was precipitated by adding an equal volume of 100% isopropanol and mixing by inversion before incubating at -20° overnight. RNA was recovered by 4° Centrifugation at 20,000 rcf for 20 min, the supernatant discarded, and the pellet washed with 80% ethanol and centrifuged at 7,500 rcf for a further 3 min. The supernatant was discarded and the pellet air-dried prior to resuspension in 50 μl DEPC-treated H$_2$O. All purified RNA was stored at -80°. RNA quantity was assessed using *ND-1000 spectrophotometer* (Nano-Drop Technologies). RNA quality was assessed using the *LabChip GXII* (Perkin-Elmer) for RIN > 6.5.

Poly(A)-enriched RNA-sequencing (mRNA-seq) libraries were prepared using the *Illumina TruSeq Stranded mRNA Sample Preparation*

Kit (Illumina, CA, USA) using 1.3 μg input of extracted total RNA. The following modifications to the manufacturer's instructions were made: reagent volumes were adjusted for 1/3 reactions; and Invitrogen SuperScript III Reverse Transcriptase (Invitrogen, Life Technologies Australia Pty Ltd) was used for first strand synthesis with adjusted reaction temperature of 50°. Libraries were constructed using *Illumina TruSeq RNA Single Indexes* (Set A and B; Illumina, CA, USA) in a 14-cycle indexing PCR reaction; all clean-ups were performed using *RNAClean XP beads* (Beckman Coulter, CA, USA). A *LabChip GXII* (Perkin Elmer, MA, USA) was used to determine library concentration and fragment size distribution, using a DNA High Sensitivity Kit. mRNA-seq libraries were pooled in equal molar ratios and sequenced (75 bp single-end) on a *NextSeq500* at the ACRF Biomolecular Research Facility (Australian National University, ACT, Australia).

Raw reads were diagnosed using *FastQC* (v0.11.2). Due to strong nucleotide sequence content bias *Trim Galore!* and *Cutadapt* were used to trim low-quality reads with PHRED score < 20 (-q 20) and to make a hard clip of 10 bp and 1 bp from the 5′ and 3′ ends, respectively. Single-end alignments of trimmed raw reads were aligned to the *TAIR10* reference genome using *Subread* (v1.6.2) (Liao *et al.* 2013) with the flags -t 0 and -u to report uniquely mapping reads, prior to sorting, indexing and compressing using *Samtools* (v1.2). Alignment metrics are provided Supplementary Dataset 3. Transcript quantification was performed at the gene-level with the *Araport11* annotation (Cheng *et al.* 2017) using *featureCounts* (with flag -s 2 for reverse strand specificity).

Differential gene expression analyses were performed using the *edgeR* quasi-likelihood pipeline (Chen *et al.* 2016). Reads mapping to ribosomal RNA and organellar transcripts were removed; only loci containing counts per million (CPM) > 1 in at least three samples were examined. After this filtering, 17,509 loci were retained for analysis. The trimmed mean of M-values (TMM) method was used to normalize transcript abundance between libraries to account for sequencing depth and composition. Diagnostic multidimensional scaling plots (*plotMDS*) revealed a lack of sample clustering into treatment groups, which suggested possible outlier samples (Figure S1 A; samples N-r3 and N+T-r3). These were omitted for subsequent analyses. Generalized linear models were fitted to estimate dispersion (*glmQLFit*) allowing for differential expression testing, employing quasi-likelihood F-tests (*glmQLTest*) and controlling for false discovery rates due to multiple hypothesis testing (FDR adjusted p-value < 0.05). Gene ontology enrichments were examined using the *statistical overrepresentation test* (Binomial test with FDR correction) from the *PANTHER* classification suite using the *Complete GO annotation datasets* (Mi *et al.* 2019). Code used for RNA-seq analyses are available on *Github* (https://goo.gl/b7x5rc).

Statistical analyses

Statistical analyses and data visualization was performed using *R* (v 3.5.0) with the *tidyverse* package (v 1.2.1). Linear mixed-effects models were fitted using the *lme4* package (v 1.1-17) (Bates *et al.* 2015) to account for both fixed (*e.g.*, genotype, condition, time) and random effects (*e.g.*, experimental design, blocking factors). Model fit was assessed using the conditional R^2 value calculated using the *piecewiseSEM* package (v 2.0.2) (Lefcheck 2016). Fitted models allowed estimation of marginal means and 95% confidence intervals using the *emmeans* package including *post hoc* contrasts between factors with FDR p-value correction (v 1.2.1). All analyses were performed on single data points, representing individual biological replicates (independent plants). Hypergeometric testing was performed using the

phyper function to test for significant overlaps, taking into account the 17,509 detected transcripts and the number of stress signaling-associated genes overlapped.

Data availability

All code used for analyses are available at *GitHub* (https://goo.gl/wsQrJT). All sequencing data generated for this study are accessible at the NCBI GEO repository (GSE121150, https://www.ncbi.nlm.nih.gov/geo/query/acc.cgi?acc=GSE121150). Independent WT and *drm1drm2* MethylC-seq profiling was accessed from GEO accessions GSE39901 and GSE38286. Supplemental material available at FigShare: https://doi.org/10.25387/g3.9724019.

RESULTS

Mutant characterization and the novel strs2 methylome

We utilized three Arabidopsis T-DNA insertion mutants targeting components of the DNA methylation machinery to test for stress priming with disrupted methylome maintenance. These include the triple methyltransferase mutant *drm1drm2cmt3* (*ddc*) (Henderson and Jacobsen 2008), the triple demethylase mutant *ros1dml2dml3* (*rdd*) (Le *et al.* 2014), and the novel putative RdDM mutant *strs2* (Khan *et al.* 2014). While *ddc* and *rdd* are well-characterized mutants displaying gross methylome changes, reports suggest that *strs2* displays subtler effects by fine-tuning DNA methylation levels at stress-associated genes (Khan *et al.* 2014). As previous studies investigating *strs2* relied on a targeted analysis using chop-PCR, we performed MethylC-seq to confirm the full extent of methylome changes. Global levels of CG, CHG, and CHH methylation in *strs2* were highly comparable to WT (Figure 1 A, Supplementary Dataset 1). However, employing *DSS* (Feng *et al.* 2014) to identify differentially methylated regions (DMRs) revealed moderate levels of local changes, predominantly in the CG context, with comparable numbers of hyper- and hypo-DMRs (Figure 1 B, Table 1, Supplementary Dataset 2). Nonetheless, many CHH DMRs were located within TEs consistent with the implication of STRS2 in RdDM. Furthermore, 130/199 (65.6%) *strs2* CHH hypo-DMRs were in regions also targeted by DRM1 and DRM2 (7,393 CHH hypo-DMRs in *drm1drm2*), whereas CG and CHG hypo-DMRs demonstrated weaker overlaps (CG: 7/318, 2.2%; CHG: 8/34, 23.5%). Paired with previous observations (Khan *et al.* 2014), our analysis confirms partial involvement of STRS2 in the RdDM pathway potentially contributing in a manner akin to prior descriptions of "weak" RdDM mutants (Stroud *et al.* 2015). However, the bias toward CG DMRs and comparable numbers of hyper- and hypo-DMRs suggests broader roles in DNA methylation patterning. Nonetheless, the *strs2* mutant fulfilled our criteria as displaying milder aberrations in DNA methylation.

Development and basal photoprotection in methylome mutants

Aberrant DNA methylation is considered to result in developmental differences due to transcriptional misregulation and TE activation; *ddc* displays curled leaves and reduced stature due to *SDC* misexpression (Henderson and Jacobsen 2008), while *strs2* shows a slight early flowering phenotype (Kant *et al.* 2007). To ensure that developmental abnormalities would not confound observations of priming, developmental traits were monitored until 4-weeks of age starting from 10-day old seedlings (Figure 2). While no unusual phenotypes were evident for *rdd* and *strs2* (Figure 2 A), *ddc* displayed the expected curled leaves after 3-weeks of age. Quantitative measures of plant area reflect these visible observations, whereby the rosette area of *ddc* was reduced compared to

A Propotion methylated cytosines along chromosome 1

— WT — *strs2*

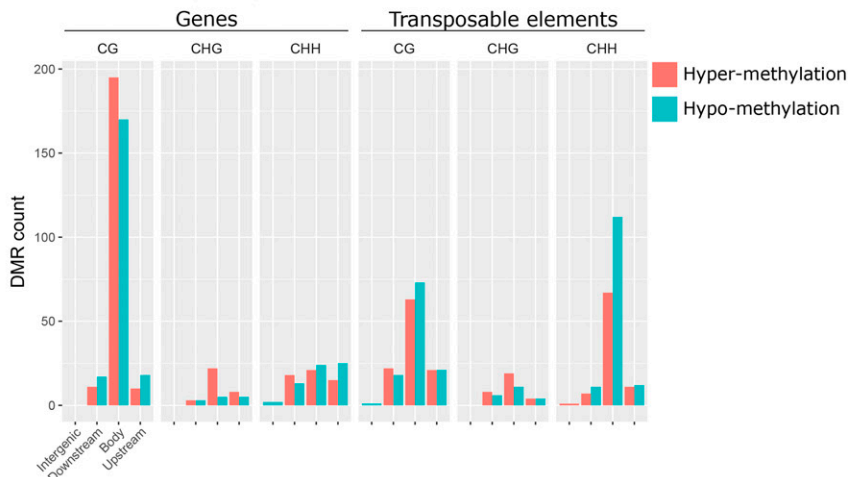**B** *strs2* DMR frequency
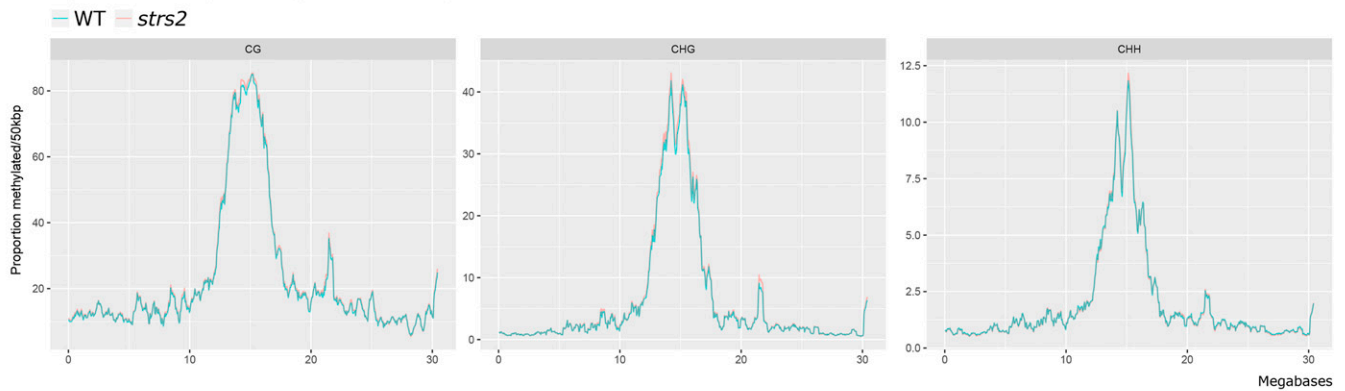
Hyper-methylation
Hypo-methylation

Figure 1 Subtle methylome perturbation in *strs2* A Mean weighted methylation levels, binned into 50 kbp rolling windows, along Arabidopsis chromosome 1 for WT and *strs2*. B DMR frequency in *strs2* grouped by genomic location relative to annotated genes or transposable elements. DMRs were classified as either occurring directly within (body), <1 kbp away from the 5` (upstream) or 3`end of (downstream), or >1 kbp (intergenic) away from genomic features.

WT (Figure 2 B). Minor differences in leaf number and plant area were observed between 3 and 4 weeks for *rdd* and *strs2*. Therefore, priming measurements were performed on 3 week-old plants prior to the onset of substantial morphological differences.

In addition to developmental abnormalities, aberrant methylome maintenance may also affect the capacity for basal photoprotective responses. Thus, functional PSII capacity was tested in 3-week old mutants (Figure 2 C). Photosynthetic efficiency (ΦPSII) was largely consistent across genotypes. Similarly, the capacity for, or activation of, actively regulated (ΦNPQ) and constitutively (ΦNO) dissipative quenching was largely consistent across genotypes. An exception to this was *rdd* that demonstrated elevated ΦNPQ with a concomitant reduction in ΦNO but unperturbed ΦPSII. However, the difference observed in *rdd* is minor compared to traditional mutants with perturbed photosystems (Niyogi *et al.* 2001) and is more reflective of

natural variation (Jung and Niyogi 2009). Thus, no major disruptions to basal PSII performance is evident in these methylation mutants allowing for comparisons of EL priming.

Excess light priming evident despite aberrant methylome patterning

To investigate whether a perturbed methylome would impair priming to recurring EL, we repeated the WLRS time-course experiment (Ganguly *et al.* 2018) on WT, *ddc*, *rdd*, and *strs2* (Figure 3). The week of recurring EL led to the expected morphological differences across all genotypes, namely increased rosette compaction but consistent leaf area (Figure 3 A-B). However, there was an attenuated difference in *ddc* area, which we attribute to its naturally curled leaf phenotype. Alongside morphological measures were changes in PSII traits indicative of physiological priming to recurring EL (Figure 3 C). The adoption of ΦNPQ and ΦNO also revealed distinct patterns in thermal dissipation not observed previously. Particularly, that the enhanced NPQ was underpinned by actively regulated pH-dependent thermal dissipation (ΦNPQ) rather than due to constitutive forms (ΦNO). Indeed, ΦNO was lower in primed plants. While ΦNPQ is rapidly activated in primed plants, it is deactivated concomitantly with an increase in ΦPSII. A key result here was that all methylation mutants demonstrated a WT-like priming response, for all three PSII traits, to recurring EL

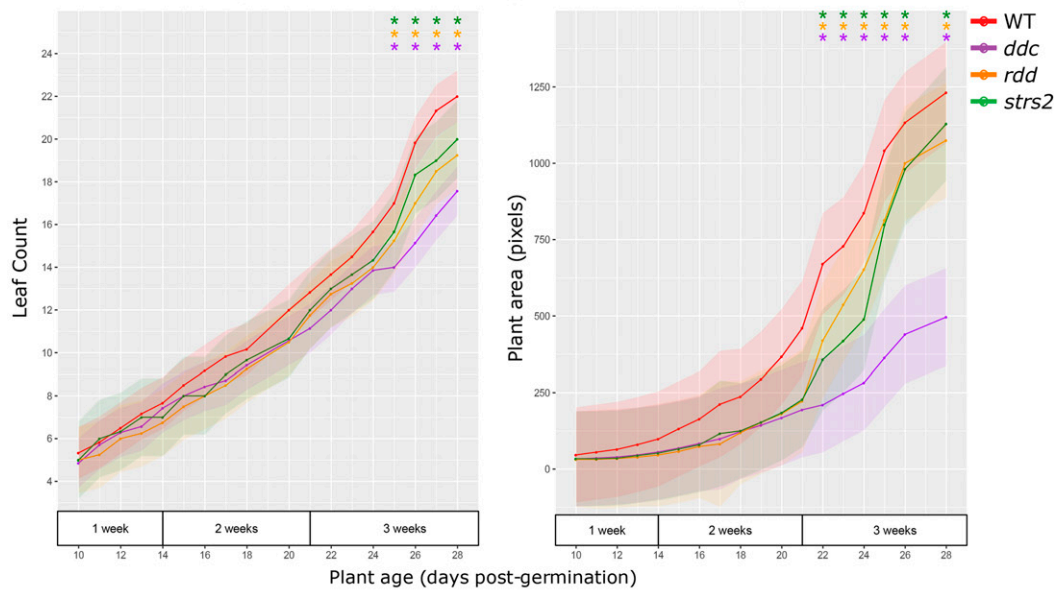■ **Table 1 DMR analysis in *strs2* (vs WT)**

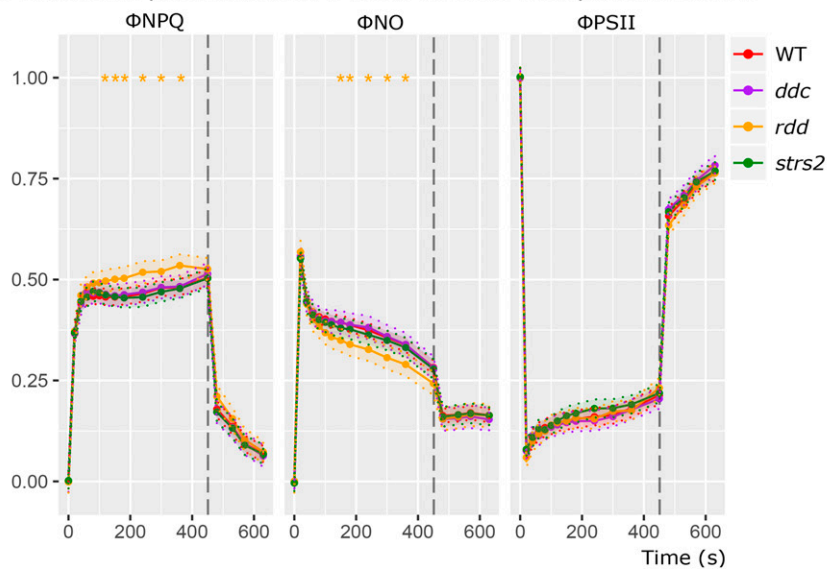| DMR type	Methylation context			
	CG	CHG	CHH	Total
Hyper-methylation	322	64	140	526
Hypo-methylation	318	34	199	551
Total	640	98	339	1,077
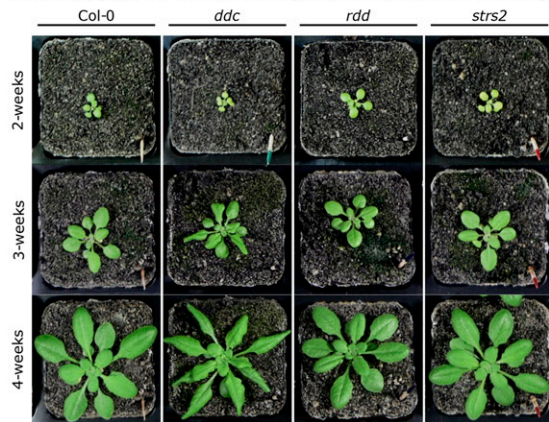
Figure 2 DNA methylation mutant development and basal PSII function A Representative morphology of WT, *ddc*, *rdd*, and *strs2* from 2-4 weeks of age. B Leaf number (left) and plant area (right) in 10-day old WT (red, n = 8), *ddc* (purple, n = 8), *rdd* (orange, n = 8), and *strs2* (green, n = 8)
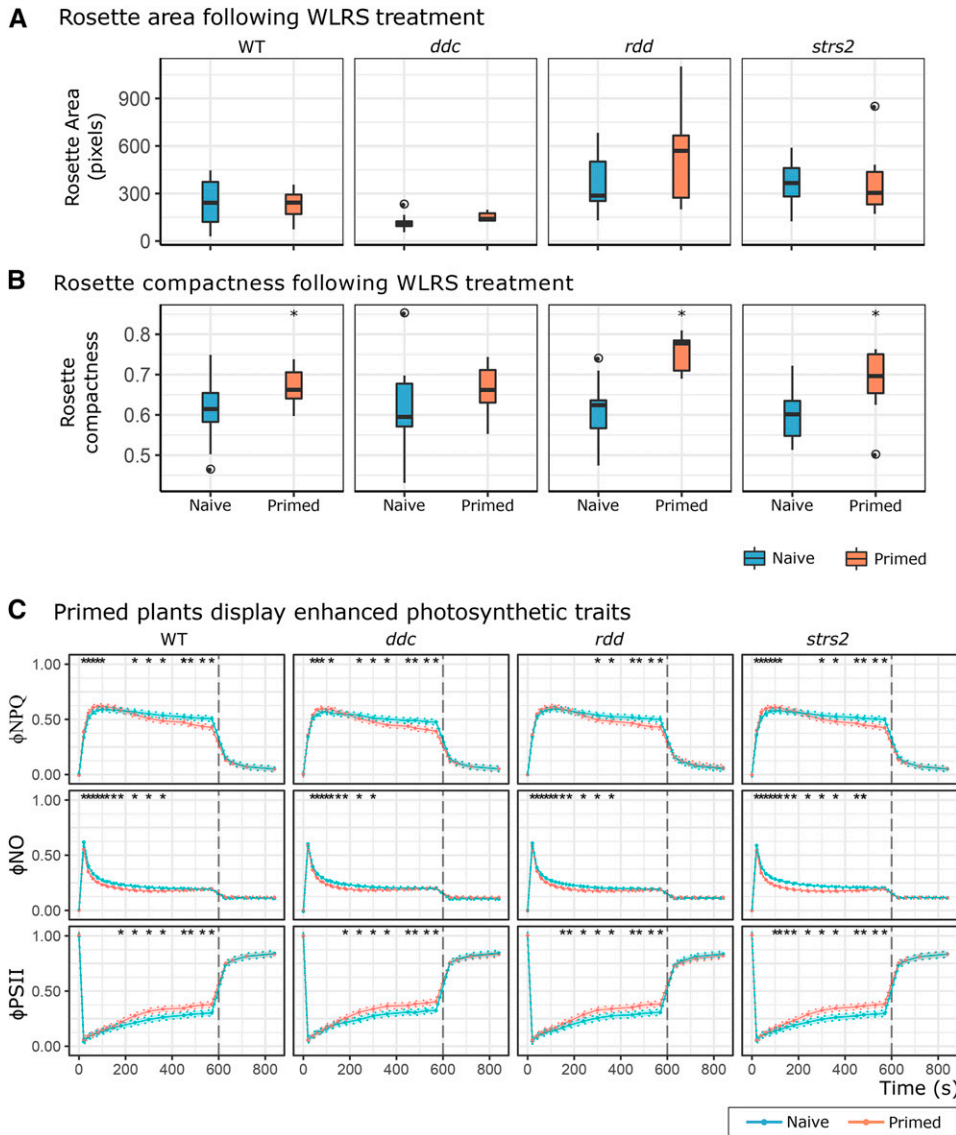
A Rosette area following WLRS treatment

B Rosette compactness following WLRS treatment

C Primed plants display enhanced photosynthetic traits

Figure 3 DNA methylation mutants exhibit priming to recurring EL A-B Boxplots of rosette area and compactness measured in all genotypes either exposed to recurring EL (primed, n = 12-15) or not (naive, 21-23). * denotes statistical significance determined using independent Student's *t*-tests for each genotype (adjusted p-value < 0.05). C PSII performance traits in naive (WT n = 22; *ddc* n = 16, *rdd* n = 21, *strs2* n = 23) and primed (WT n = 16; *ddc* n = 13, *rdd* n = 12, *strs2* n = 15) plants for all genotypes. Points denote estimated marginal means based on a fitted linear mixed-effect model for each genotype. Bars and shading denote 95% confidence intervals; * indicates statistical significance (adjusted p-value < 0.05) from WT.
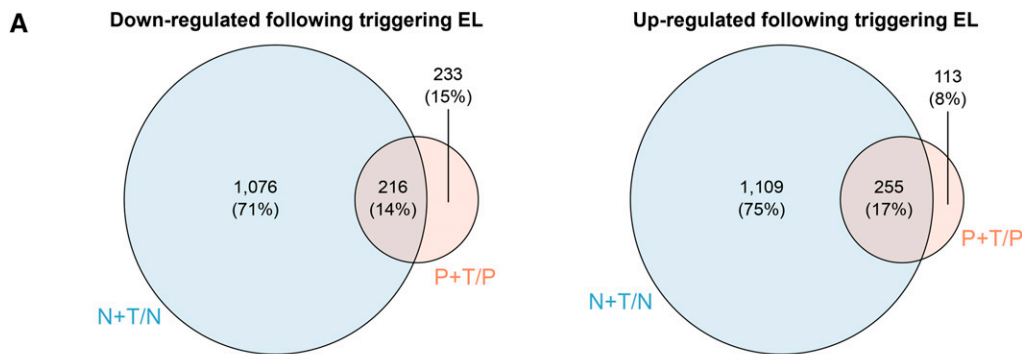
thus demonstrating appropriate light-acclimatory processes despite having perturbed methylomes.

Primed plants exhibit transcriptional 'dampening' despite a reset transcriptome

Persistent changes in gene expression are hypothesized to convey a primed state (Hilker *et al.* 2016). To test this, we searched for constitutive changes in gene expression between naïve (N) and primed (P) plants after one-week of recurring EL using mRNA-seq. Despite the observation of physiological priming in these tissues, we observed a completely reset transcriptome exemplified by close sample clustering and the absence of differentially expressed genes (DEGs) between naïve and primed samples (Figure S1 A-B). We subsequently investigated the

transcriptional response of primed plants to an additional EL treatment (triggering stress, P+T). Application of an EL triggering stress to naive plants (N+T) elicited the differential expression of hundreds of genes, however, primed plants showed a vastly attenuated response (Figure S1 C-D, Supplementary Datasets 4 - 5). While the majority of EL-induced transcripts in P+T plants overlapped with those in N+T plants, a striking proportion of both up- (75%) and down-regulated (71%) transcripts were unique to N+T plants (Figure 4 A). The abundance of nearly all 1,076 uniquely down-regulated transcripts in N+T plants was greater in P+T plants (Figure 4 B, left). Equivalently, abundance of the 1,109 uniquely up-regulated transcripts in N+T plants was decreased in P+T plants (Figure 4 B, right). Together, these results evoke a dampened transcriptional response to EL triggering stimuli in

seedlings, monitored for 20 days until 4-weeks of age. C Measures of PSII performance in 3-week old WT (red, n = 60), *ddc* (purple, n = 10), *rdd* (orange, n = 10), *strs2* (green, n = 15) plants grown under standard conditions. Points denote estimated marginal means based on a fitted linear mixed-effect model for each genotype. Bars and shaded regions denote 95% confidence intervals; * indicates statistical significance (adjusted p-value < 0.05) from WT.

A

Down-regulated following triggering EL

233
(15%)

1,076
(71%)   216
(14%)

N+T/N   P+T/P

Up-regulated following triggering EL

113
(8%)

1,109
(75%)   255
(17%)

N+T/N   P+T/P

B **Abundance of uniquely up- and down-regulated transcripts in N + T (dampened transcripts)**

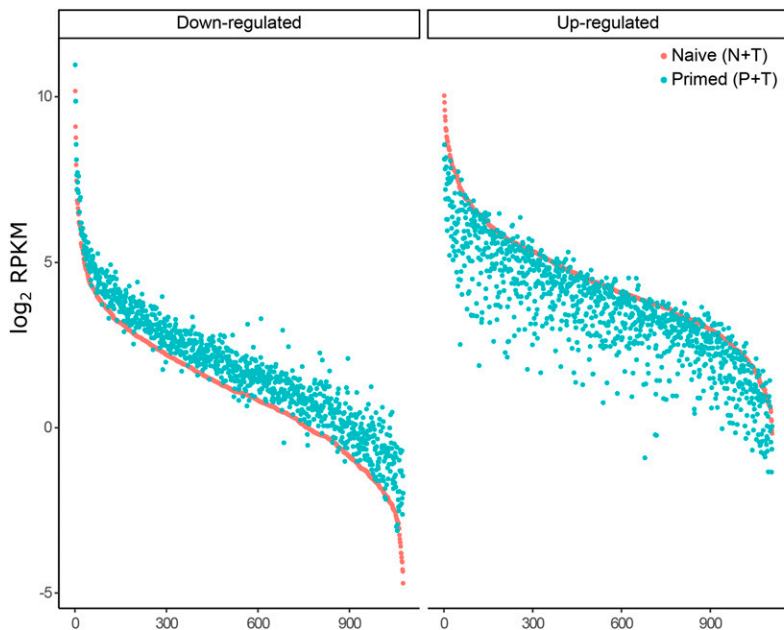Down-regulated   Up-regulated

• Naive (N+T)
• Primed (P+T)

Figure 4 Transcriptional 'damp-ening' evident in EL primed plants A Overlap between up- and down-regulated transcripts in naive and primed plants in response to an additional triggering EL treatment. B Transcript abundance ($\log_2$ RPKM) of up- (left) and down-regulated (right) transcripts, in N+T plants, for both N+T and P+T plants.

primed plants, rather than reflecting differences between their basal (un-triggered) transcriptomes. The dampening effect is, however, subtle in nature - no DEGs were identified upon direct comparison of N+T and P+T samples.

We hypothesized that the transcriptional dampening observed in primed plants may be a consequence of reduced stress signaling because of enhanced dissipative quenching (Rossel *et al.* 2007; Suzuki *et al.* 2013; Carmody *et al.* 2016). A gene ontology analysis of the 2,185 dampened transcripts (Supplementary Dataset 6) revealed a strong enrichment for terms associated with various catabolic processes (*e.g.*, protein, cellulose, and fatty acid catabolism) and, pertinent to our hypothesis, numerous stress factors, including salt, heat, water deprivation, and metal ion (Supplementary Dataset 7). Subsequently, genes induced by well-established stress signals including ROS (hydrogen peroxide [H_2O_2], singlet oxygen [$^1O_2$], and superoxide [O_2^-] (Gadjev *et al.* 2006)), salicylic acid (SA) (Blanco *et al.* 2009), β-cyclocitral (Ramel *et al.* 2012), ABA (Pornsiriwong *et al.* 2017), and SAA (Rossel *et al.* 2007) were overlapped with the dampened transcripts identified here. In total, 635/2,185 (29.1%) dampened transcripts were overlapped with the collated gene list. Performing hypergeometric testing on a per signal basis revealed statistically significant overlaps with β-cyclocitral and SAA induced genes (Table 2).

DISCUSSION

The popular notion that DNA methylation may regulate plant stress responses is confounded by both supporting and conflicting investigations spanning a range of species and stressors. Light stress is one such example for which physiological priming and memory have been demonstrated in Arabidopsis (Szechyńska-Hebda *et al.* 2010; Gordon *et al.* 2012), yet we did not observe co-occurring stress-induced DNA methylation changes (Ganguly *et al.* 2018). Consequently, we refined the experimental design to address a distinct

■ **Table 2 Hypergeometric testing of 2,185 dampened transcripts overlapped with genes responsive to stress signals**

Gene list	Total responsive genes	Overlap with dampened transcripts	Hypergeometric test
ABA	2,471	252	$P_{[X \geq 252]} = 0.99$
SA	217	21	$P_{[X \geq 21]} = 0.88$
O_2^-	209	7	$P_{[X \geq 7]} = 0.99$
H_2O_2	325	36	$P_{[X \geq 36]} = 0.75$
$^1O_2$	295	19	$P_{[X \geq 19]} = 0.99$
β-cyclocitral	1,145	191	$P_{[X \geq 191]} < 0.001$
SAA	703	109	$P_{[X \geq 109]} < 0.001$

■ Table 3 Diagnostic PSII parameters and their biological relevance

Parameter	Equation	Interpretation
ΦPSII	$1 - F_t/F_m{}'$	Fraction of light absorbed by PSII for photochemistry.
ΦNPQ	$F_t/F_m{}' - F_t/F_m{}'$	Fraction of light absorbed by PSII that is lost via thermal dissipation (ΔpH- and xanthophyll-regulated processes).
ΦNPQ	F_t/F_m	Fraction of light absorbed by PSII that is lost via chlorophyll fluorescence.

hypothesis: that physiological priming of recurring EL is underpinned by transcriptional regulation for which active maintenance of DNA methylation is important. We present evidence for recurring EL priming in DNA methylation mutants using a full-factorial experimental design, which facilitated systematic testing of two closely related potential priming mechanisms: 1. DNA methylation-mediated transcriptional regulation; and 2. altered transcription (independent of DNA methylation).

DNA methylation, development, and priming

Loss of DNA methylation leads to abnormal plant growth due to its importance for genome integrity (Reinders *et al.* 2009). Abnormal leaf development could in turn lead to confounding changes in light acclimation that are not a direct result of DNA methylation changes to light stress-responsive genes. Thus, we performed detailed physiological characterization of DNA methylation mutants to identify any constitutive changes in photosynthetic rate or capacity that could confound our interpretation of the contribution of DNA methylation to priming. Irrespective of the nature of methylome perturbance, we found negligible changes in photosynthesis at the developmental stage examined here.

We utilized two well-characterized methylation mutants, *ddc* and *rdd*, which display genome-wide hypomethylation and hypermethylation, respectively (Stroud *et al.* 2014, 2015). These relatively severe mutants were complemented by *strs2*, included based on reports of disrupted RdDM leading to targeted methylation changes at stress-responsive genes (Kant *et al.* 2007; Khan *et al.* 2014). While our focused analysis confirmed some contribution of STRS2 toward RdDM, our global analysis suggests a broader function and confirmed the relatively mild nature of the *strs2* methylome in comparison to *ddc* and *rdd*.

Light stress induces multiple physiological, post-transcriptional and extensive transcriptional responses (Dietz 2015). Thus, it was hypothesized that changes in DNA methylation might impact the transcriptional component of the acclimation response, thereby impairing the ability for EL priming. Contradictory to this hypothesis perturbation of the methylome, regardless of severity (*e.g.*, *strs2 vs. ddc*) or type (*e.g.*, hyper- or hypo-methylation), did not impair basal photoprotective capacity nor the ability to be primed by recurring EL. Instead, the EL priming observed herein likely reflects post-transcriptional changes of the photosynthetic machinery. The reduction in ΦNO disputes constitutive changes in PSII conformation. Rather there appears to be greater electron flow (increased ΦPSII) in primed plants that may reflect an increased concentration of components facilitating photosynthetic electron transport, such as PSII core proteins, cytochrome b_6f, and chloroplastic ATPases (Foyer *et al.* 2012; Dwyer *et al.* 2012; Zhu *et al.* 2017). Pertinent to this study is the observation that these processes remain functional under a range of methylome perturbations (Table 3).

Priming occurs independently of transcriptional changes

Transcriptional up-regulation of light-responsive genes is indicative of an acclimatory response (Gordon *et al.* 2012; Carmody *et al.* 2016), however, it remains an untested hypothesis that EL priming is underpinned by constitutive transcriptional changes. No persistent changes in gene expression were observed in primed plants, consistent with previous reports of transcriptome resetting following EL exposure (Crisp *et al.* 2017). Instead, an attenuated transcriptional response ("transcriptional dampening") was observed in primed plants responding to a final triggering stress. This contrasts enhanced transcriptional responses observed upon a triggering stimulus following single stress treatments (Ding *et al.* 2012; Lämke *et al.* 2016; Crisp *et al.* 2017). The transcriptional dampening observed likely reflects a greater capacity of primed plants, after longer-term recurring EL exposure, to deal with increased light flux. That is, enhanced photosynthetic and photoprotective capacity in primed plants may alter the extent of EL-mediated signaling leading to an attenuated response. Indeed, nuclear gene expression can be modulated by changes in photosynthetic electron flow that can subsequently affect cellular metabolism and acclimatory responses (Gollan *et al.* 2017; Dickinson *et al.* 2018). Taken together, we propose that the dampened transcriptional response might be a consequence of altered stress signaling due to physiological priming. In support of this hypothesis was the observation that almost one-third of dampened transcripts overlapped with genes responsive to signaling pathways, specifically β-cyclocitral and SAA. However, limitations of the analysis performed here are that these signals were not directly assayed and they do not account for all dampened transcripts. Nonetheless, these results suggest that the gene expression changes observed in primed plants are consequential of physiological priming, rather than the cause.

Conclusion

Through the analysis of Arabidopsis mutants impaired in active methylome maintenance, we have conducted a systematic investigation of the hypothesis that DNA methylation may contribute to stress priming. Specifically, we address the hypothesis that physiological priming to recurring EL is underpinned by transcriptional regulation and active methylome maintenance. We found no evidence to suggest that aberrant maintenance or removal of DNA methylation impaired the capacity for physiological priming against recurring EL. In fact, primed plants demonstrated completely reset transcriptomes. Instead, an attenuation in transcriptional response to EL was observed in primed plants and is likely to be a consequence rather than a cause of physiological priming.

LITERATURE CITED

Allen, R. S., J. Li, M. M. Alonso-Peral, R. G. White, F. Gubler *et al.*, 2010 MicroR159 regulation of most conserved targets in Arabidopsis has negligible phenotypic effects. Silence 1: 18. https://doi.org/10.1186/1758-907X-1-18

Baker, N. R., 2008   Chlorophyll fluorescence: a probe of photosynthesis in vivo. Annu. Rev. Plant Biol. 59: 89–113. https://doi.org/10.1146/annurev.arplant.59.032607.092759

Bates, D., M. Mächler, B. Bolker, and S. Walker, 2015   Fitting Linear Mixed-Effects Models Using lme4. J. Stat. Softw. 67: 1–48.

Bewick, A. J., L. Ji, C. E. Niederhuth, E.-M. Willing, B. T. Hofmeister et al., 2016   On the origin and evolutionary consequences of gene body DNA methylation. Proc. Natl. Acad. Sci. USA 113: 9111–9116. https://doi.org/10.1073/pnas.1604666113

Blanco, F., P. Salinas, N. M. Cecchini, X. Jordana, P. Van Hummelen et al., 2009   Early genomic responses to salicylic acid in Arabidopsis. Plant Mol. Biol. 70: 79–102. https://doi.org/10.1007/s11103-009-9458-1

Boyko, A., T. Blevins, Y. Yao, A. Golubov, A. Bilichak et al., 2010   Transgenerational Adaptation of Arabidopsis to Stress Requires DNA Methylation and the Function of Dicer-Like Proteins. PLoS One 5: e9514.

Carmody, M., P. A. Crisp, S. d'Alessandro, D. Ganguly, M. Gordon et al., 2016   Uncoupling High Light Responses from Singlet Oxygen Retrograde Signaling and Spatial-Temporal Systemic Acquired Acclimation. Plant Physiol. 171: 1734–1749. https://doi.org/10.1104/pp.16.00404

Cheng, C.-Y., V. Krishnakumar, A. P. Chan, F. Thibaud-Nissen, S. Schobel et al., 2017   Araport11: a complete reannotation of the Arabidopsis thaliana reference genome. Plant J. 89: 789–804. https://doi.org/10.1111/tpj.13415

Chen, Y., A. T. L. Lun, and G. K. Smyth, 2016   From reads to genes to pathways: differential expression analysis of RNA-Seq experiments using Rsubread and the edgeR quasi-likelihood pipeline. F1000 Res. 5: 1438.

Cokus, S. J., S. Feng, X. Zhang, Z. Chen, B. Merriman et al., 2008   Shotgun bisulphite sequencing of the Arabidopsis genome reveals DNA methylation patterning. Nature 452: 215–219. https://doi.org/10.1038/nature06745

Cortijo, S., R. Wardenaar, M. Colomé-Tatché, A. Gilly, M. Etcheverry et al., 2014   Mapping the epigenetic basis of complex traits. Science 343: 1145–1148. https://doi.org/10.1126/science.1248127

Crisp, P. A., D. R. Ganguly, A. B. Smith, K. D. Murray, G. M. Estavillo et al., 2017   Rapid Recovery Gene Downregulation during Excess-Light Stress and Recovery in Arabidopsis. Plant Cell 29: 1836–1863. https://doi.org/10.1105/tpc.16.00828

Dickinson, P. J., M. Kumar, C. Martinho, S. J. Yoo, H. Lan et al., 2018   Chloroplast Signaling Gates Thermotolerance in Arabidopsis. Cell Reports 22: 1657–1665. https://doi.org/10.1016/j.celrep.2018.01.054

Dietz, K.-J., 2015   Efficient high light acclimation involves rapid processes at multiple mechanistic levels. J. Exp. Bot. 66: 2401–2414. https://doi.org/10.1093/jxb/eru505

Ding, Y., M. Fromm, and Z. Avramova, 2012   Multiple exposures to drought "train" transcriptional responses in Arabidopsis. Nat. Commun. 3: 740. https://doi.org/10.1038/ncomms1732

Dwyer, S. A., W. S. Chow, W. Yamori, J. R. Evans, S. Kaines et al., 2012   Antisense reductions in the PsbO protein of photosystem II leads to decreased quantum yield but similar maximal photosynthetic rates. J. Exp. Bot. 63: 4781–4795. https://doi.org/10.1093/jxb/ers156

Feng, H., K. N. Conneely, and H. Wu, 2014   A Bayesian hierarchical model to detect differentially methylated loci from single nucleotide resolution sequencing data. Nucleic Acids Res. 42: e69. https://doi.org/10.1093/nar/gku154

Finnegan, E. J., W. J. Peacock, and E. S. Dennis, 1996   Reduced DNA methylation in Arabidopsis thaliana results in abnormal plant development. Proc. Natl. Acad. Sci. USA 93: 8449–8454. https://doi.org/10.1073/pnas.93.16.8449

Foyer, C. H., J. Neukermans, G. Queval, G. Noctor, and J. Harbinson, 2012   Photosynthetic control of electron transport and the regulation of gene expression. J. Exp. Bot. 63: 1637–1661. https://doi.org/10.1093/jxb/ers013

Gadjev, I., S. Vanderauwera, T. S. Gechev, C. Laloi, I. N. Minkov et al., 2006   Transcriptomic footprints disclose specificity of reactive oxygen species signaling in Arabidopsis. Plant Physiol. 141: 436–445. https://doi.org/10.1104/pp.106.078717

Ganguly, D. R., P. A. Crisp, S. R. Eichten, and B. J. Pogson, 2018   Maintenance of pre-existing DNA methylation states through recurring excess-light stress. Plant Cell Environ. 41: 1657–1672. https://doi.org/10.1111/pce.13324

Gollan, P. J., Y. Lima-Melo, A. Tiwari, M. Tikkanen, and E.-M. Aro, 2017   Interaction between photosynthetic electron transport and chloroplast sinks triggers protection and signalling important for plant productivity. Philos. Trans. R. Soc. Lond. B Biol. Sci. 372: 1730. https://doi.org/10.1098/rstb.2016.0390

Gordon, M. J., M. Carmody, V. Albrecht, and B. Pogson, 2012   Systemic and Local Responses to Repeated HL Stress-Induced Retrograde Signaling in Arabidopsis. Front. Plant Sci. 3: 303.

Henderson, I. R., and S. E. Jacobsen, 2008   Tandem repeats upstream of the Arabidopsis endogene SDC recruit non-CG DNA methylation and initiate siRNA spreading. Genes Dev. 22: 1597–1606. https://doi.org/10.1101/gad.1667808

Hendrickson, L., R. T. Furbank, and W. S. Chow, 2004   A simple alternative approach to assessing the fate of absorbed light energy using chlorophyll fluorescence. Photosynth. Res. 82: 73–81. https://doi.org/10.1023/B:PRES.0000040446.87305.f4

He, L., W. Wu, G. Zinta, L. Yang, D. Wang et al., 2018   A naturally occurring epiallele associates with leaf senescence and local climate adaptation in Arabidopsis accessions. Nat. Commun. 9: 460. https://doi.org/10.1038/s41467-018-02839-3

Hilker, M., J. Schwachtje, M. Baier, S. Balazadeh, I. Bäurle et al., 2016   Priming and memory of stress responses in organisms lacking a nervous system. Biol. Rev. Camb. Philos. Soc. 91: 1118–1133. https://doi.org/10.1111/brv.12215

Iwasaki, M., and J. Paszkowski, 2014   Identification of genes preventing transgenerational transmission of stress-induced epigenetic states. Proc. Natl. Acad. Sci. USA 111: 8547–8552. https://doi.org/10.1073/pnas.1402275111

Johannes, F., E. Porcher, F. K. Teixeira, V. Saliba-Colombani, M. Simon et al., 2009   Assessing the impact of transgenerational epigenetic variation on complex traits. PLoS Genet. 5: e1000530. https://doi.org/10.1371/journal.pgen.1000530

Johannes, F., and R. J. Schmitz, 2019   Spontaneous epimutations in plants. New Phytol. 221: 1253–1259. https://doi.org/10.1111/nph.15434

Jung, H.-S., and K. K. Niyogi, 2009   Quantitative genetic analysis of thermal dissipation in Arabidopsis. Plant Physiol. 150: 977–986. https://doi.org/10.1104/pp.109.137828

Kant, P., S. Kant, M. Gordon, R. Shaked, and S. Barak, 2007   STRESS RESPONSE SUPPRESSOR1 and STRESS RESPONSE SUPPRESSOR2, two DEAD-box RNA helicases that attenuate Arabidopsis responses to multiple abiotic stresses. Plant Physiol. 145: 814–830. https://doi.org/10.1104/pp.107.099895

Karpinski, S., 1999   Systemic Signaling and Acclimation in Response to Excess Excitation Energy in Arabidopsis. Science 284: 654–657. https://doi.org/10.1126/science.284.5414.654

Khan, A., A. Garbelli, S. Grossi, A. Florentin, G. Batelli et al., 2014   The Arabidopsis STRESS RESPONSE SUPPRESSOR DEAD-box RNA helicases are nucleolar- and chromocenter-localized proteins that undergo stress-mediated relocalization and are involved in epigenetic gene silencing. Plant J. 79: 28–43. https://doi.org/10.1111/tpj.12533

Kim, J.-M., T. K. To, A. Matsui, K. Tanoi, N. I. Kobayashi et al., 2017   Acetate-mediated novel survival strategy against drought in plants. Nat. Plants 3: 17097. Erratum: 17097. https://doi.org/10.1038/nplants.2017.97

Kramer, D. M., G. Johnson, O. Kiirats, and G. E. Edwards, 2004   New Fluorescence Parameters for the Determination of QARedox State and Excitation Energy Fluxes. Photosynth. Res. 79: 209–218. https://doi.org/10.1023/B:PRES.0000015391.99477.0d

Krueger, F., and S. R. Andrews, 2011   Bismark: a flexible aligner and methylation caller for Bisulfite-Seq applications. Bioinformatics 27: 1571–1572. https://doi.org/10.1093/bioinformatics/btr167

Lämke, J., K. Brzezinka, S. Altmann, and I. Bäurle, 2016   A hit-and-run heat shock factor governs sustained histone methylation and transcriptional

stress memory. EMBO J. 35: 162–175. https://doi.org/10.15252/embj.201592593

Langmead, B., and S. L. Salzberg, 2012 Fast gapped-read alignment with Bowtie 2. Nat. Methods 9: 357–359. https://doi.org/10.1038/nmeth.1923

Lefcheck, J. S., 2016 PIECEWISESEM: Piecewise structural equation modelling in r for ecology, evolution, and systematics. Methods Ecol. Evol. 7: 573–579.

Le, T.-N., U. Schumann, N. A. Smith, S. Tiwari, P. C. K. Au et al., 2014 DNA demethylases target promoter transposable elements to positively regulate stress responsive genes in Arabidopsis. Genome Biol. 15: 458. https://doi.org/10.1186/s13059-014-0458-3

Liao, Y., G. K. Smyth, and W. Shi, 2013 The Subread aligner: fast, accurate and scalable read mapping by seed-and-vote. Nucleic Acids Res. 41: e108. https://doi.org/10.1093/nar/gkt214

Matzke, M. A., and R. A. Mosher, 2014 RNA-directed DNA methylation: an epigenetic pathway of increasing complexity. Nat. Rev. Genet. 15: 394–408. Erratum: 570. https://doi.org/10.1038/nrg3683

Meng, D., M. Dubin, P. Zhang, E. J. Osborne, O. Stegle et al., 2016 Limited Contribution of DNA Methylation Variation to Expression Regulation in Arabidopsis thaliana. PLoS Genet. 12: e1006141. https://doi.org/10.1371/journal.pgen.1006141

Mi, H., A. Muruganujan, X. Huang, D. Ebert, C. Mills et al., 2019 Protocol Update for large-scale genome and gene function analysis with the PANTHER classification system (v.14.0). Nat. Protoc. 14: 703–721. https://doi.org/10.1038/s41596-019-0128-8

Molloy, P. L., 1986 Effects of DNA methylation on specific transcription by RNA polymerase II in vitro. Mol. Biol. Rep. 11: 13–17. https://doi.org/10.1007/BF00417589

Muyle, A., and B. S. Gaut, 2019 Loss of gene body methylation in Eutrema salsugineum is associated with reduced gene expression. Mol. Biol. Evol. 36: 155–158. https://doi.org/10.1093/molbev/msy204

Niyogi, K. K., C. Shih, W. Soon Chow, B. J. Pogson, D. DellaPenna et al., 2001 Photosynth. Res. 67: 139–145. https://doi.org/10.1023/A:1010661102365

O'Malley, R. C., S.-S. C. Huang, L. Song, M. G. Lewsey, A. Bartlett et al., 2016 Cistrome and Epicistrome Features Shape the Regulatory DNA Landscape. Cell 165: 1280–1292. Erratum: 1598. https://doi.org/10.1016/j.cell.2016.04.038

Ong-Abdullah, M., J. M. Ordway, N. Jiang, S.-E. Ooi, S.-Y. Kok et al., 2015 Loss of Karma transposon methylation underlies the mantled somaclonal variant of oil palm. Nature 525: 533–537. https://doi.org/10.1038/nature15365

Pornsiriwong, W., G. M. Estavillo, K. X. Chan, E. E. Tee, D. Ganguly et al., 2017 A chloroplast retrograde signal, 3′-phosphoadenosine 5′-phosphate, acts as a secondary messenger in abscisic acid signaling in stomatal closure and germination. eLife 6: 1–34. https://doi.org/10.7554/eLife.23361

Quinlan, A. R., and I. M. Hall, 2010 BEDTools: a flexible suite of utilities for comparing genomic features. Bioinformatics 26: 841–842. https://doi.org/10.1093/bioinformatics/btq033

Ramel, F., S. Birtic, C. Ginies, L. Soubigou-Taconnat, C. Triantaphylidès et al., 2012 Carotenoid oxidation products are stress signals that mediate gene responses to singlet oxygen in plants. Proc. Natl. Acad. Sci. USA 109: 5535–5540. https://doi.org/10.1073/pnas.1115982109

Reinders, J., B. B. H. Wulff, M. Mirouze, A. Marí-Ordóñez, M. Dapp et al., 2009 Compromised stability of DNA methylation and transposon immobilization in mosaic Arabidopsis epigenomes. Genes Dev. 23: 939–950. https://doi.org/10.1101/gad.524609

Rossel, J. B., P. B. Wilson, D. Hussain, N. S. Woo, M. J. Gordon et al., 2007 Systemic and intracellular responses to photooxidative stress in Arabidopsis. Plant Cell 19: 4091–4110. https://doi.org/10.1105/tpc.106.045898

Rowley, M. J., M. H. Rothi, G. Böhmdorfer, J. Kuciński, and A. T. Wierzbicki, 2017 Long-range control of gene expression via RNA-directed DNA methylation. PLoS Genet. 13: e1006749. https://doi.org/10.1371/journal.pgen.1006749

Sani, E., P. Herzyk, G. Perrella, V. Colot, and A. Amtmann, 2013 Hyperosmotic priming of Arabidopsis seedlings establishes a long-term somatic memory accompanied by specific changes of the epigenome. Genome Biol. 14: R59. https://doi.org/10.1186/gb-2013-14-6-r59

Schultz, M. D., R. J. Schmitz, and J. R. Ecker, 2012 "Leveling" the playing field for analyses of single-base resolution DNA methylomes. Trends Genet. 28: 583–585. https://doi.org/10.1016/j.tig.2012.10.012

Secco, D., C. Wang, H. Shou, M. D. Schultz, S. Chiarenza et al., 2015 Stress induced gene expression drives transient DNA methylation changes at adjacent repetitive elements. eLife 4: 1–26. https://doi.org/10.7554/eLife.09343

Shukla, S., E. Kavak, M. Gregory, M. Imashimizu, B. Shutinoski et al., 2011 CTCF-promoted RNA polymerase II pausing links DNA methylation to splicing. Nature 479: 74–79. https://doi.org/10.1038/nature10442

Stroud, H., T. Do, J. Du, X. Zhong, S. Feng et al., 2014 Non-CG methylation patterns shape the epigenetic landscape in Arabidopsis. Nat. Struct. Mol. Biol. 21: 64–72. https://doi.org/10.1038/nsmb.2735

Stroud, H., M. V. C. Greenberg, S. Feng, Y. V. Bernatavichute, and S. E. Jacobsen, 2015 Comprehensive Analysis of Silencing Mutants Reveals Complex Regulation of the Arabidopsis Methylome. Cell 161: 1697–1698. Erratum: 1697–1698. https://doi.org/10.1016/j.cell.2015.06.020

Suzuki, N., G. Miller, C. Salazar, H. A. Mondal, E. Shulaev et al., 2013 Temporal-spatial interaction between reactive oxygen species and abscisic acid regulates rapid systemic acclimation in plants. Plant Cell 25: 3553–3569. https://doi.org/10.1105/tpc.113.114595

Szechyńska-Hebda, M., J. Kruk, M. Górecka, B. Karpińska, and S. Karpiński, 2010 Evidence for light wavelength-specific photoelectrophysiological signaling and memory of excess light episodes in Arabidopsis. Plant Cell 22: 2201–2218. https://doi.org/10.1105/tpc.109.069302

Wibowo, A., C. Becker, G. Marconi, J. Durr, J. Price et al., 2016 Hyperosmotic stress memory in Arabidopsis is mediated by distinct epigenetically labile sites in the genome and is restricted in the male germline by DNA glycosylase activity. eLife 5: e13546. https://doi.org/10.7554/eLife.13546

Williams, B. P., and M. Gehring, 2017 Stable transgenerational epigenetic inheritance requires a DNA methylation-sensing circuit. Nat. Commun. 8: 2124. https://doi.org/10.1038/s41467-017-02219-3

Wu, H., T. Xu, H. Feng, L. Chen, B. Li et al., 2015 Detection of differentially methylated regions from whole-genome bisulfite sequencing data without replicates. Nucleic Acids Res. 43: e141.

Yin, Y., E. Morgunova, A. Jolma, E. Kaasinen, B. Sahu et al., 2017 Impact of cytosine methylation on DNA binding specificities of human transcription factors. Science 356: eaaj2239. https://doi.org/10.1126/science.aaj2239

Zhu, H., L.-D. Zeng, X.-P. Yi, C.-L. Peng, W.-F. Zhang et al., 2017 The half-life of the cytochrome bf complex in leaves of pea plants after transfer from moderately-high growth light to low light. Funct. Plant Biol. 44: 351. https://doi.org/10.1071/FP16222

Communicating editor: B. Gregory